RESEARCH ARTICLE

Lipid Oxidation

European Journal of Lipid Science and Technology

www.ejlst.com

GC-MS Characterization of Hydroxy Fatty Acids Generated From Lipid Oxidation in Vegetable Oils

Wei Xia and Suzanne M. Budge*

Lipid oxidation has long been described as following a radical chain reaction mechanism, where hydrogen abstraction is considered the preferred pathway. Hydroxy compounds are, in theory, major products formed from hydrogen abstraction but their presence is rarely monitored. In this study, a GC-MS technique to characterize hydroxy fatty acids (FA) formed during the oxidation of sunflower and canola oils is described. First, hydroxy FA in oxidized oils are methylated and isolated from non-oxygenated structures using solid phase extraction (SPE). Then they are converted into their trimethylsilyl (TMS) derivatives using a N,O-bis (trimethylsilyl) trifluoroacetamide (BSTFA)-pyridine method and identified by their electron ionization (EI) and positive chemical ionization (PCI) spectra. Separation of most isomeric hydroxy FA with very similar structures is accomplished using a DB-23 capillary column with (50%-cyanopropyl)-methylpolysiloxane phase. The fragmentation patterns of the TMS derivatives are discussed in detail and several easily applicable rules for spectral interpretations are presented. The major hydroxy FA arising from oxidation of sunflower and canola oils are allylic and conjugated structures, specifically 8-, 9-, 10-, and 11-hydroxyoctadecenoic acid (OH-C18:1) and 9- and 13-hydroxyoctadecadienoic acid (OH-C18:2).

***Practical Applications*: Unsaturated hydroxy FA are potential indicators of hydrogen abstraction reactions by FA alkoxyl radicals during lipid oxidation. A prerequisite for the quantification of these hydroxy FA is knowledge of their structures. In this work a GC-MS method, coupled with SPE and TMS derivatization, to characterize the hydroxy FA derived from oxidation of vegetable oils, which will enable future quantifications of these compounds is employed. In addition, the use of EI and PCI spectra provided clear strategies to interpret mass spectra for both saturated and unsaturated hydroxy FA. The fragmentation patterns in EI and PCI presented in this paper will benefit future studies on identification or quantification of both saturated and unsaturated hydroxy FA in other lipid samples.**

1. Introduction

For decades, lipid autoxidation has been thought to follow a radical chain reaction mechanism, which includes the initiation, propagation, and termination stages.[1] In the initiation stage, radicals form from lipid molecules in the presence of initiators such as light, heat, and metals.[2] Oxygen is then added to lipid radicals which in turn form peroxyl radicals in the propagation step. Peroxyl radicals can abstract hydrogen atoms from other lipid molecules, generating new lipid radicals and hydroperoxides. The new lipid radicals formed can then participate in further chain reactions. The hydroperoxides produced at this stage are considered primary oxidation products and important intermediates; thus, they break down and produce alkoxyl radicals. This reaction scheme suggests that hydrogen abstraction is the preferred pathway in the chain reaction, so hydroxy compounds formed through hydrogen abstraction by alkoxyl radicals should also be major products. However, the effectiveness of this reaction is believed to be limited by other pathways, such as cyclization and scission of alkoxyl radicals.[3]

Compared to the large number of studies on hydroperoxides, literature reports of the formation of hydroxy FA are rare. Preliminary studies on the formation of hydroxy FA were conducted through decomposition of FA hydroperoxide standards.[4–6] In more recent years, quantitative studies of hydroxy FA in oxidized edible oils have been carried out with GC approaches, which exhibited excellent accuracy and sensitivity.[7,8] Methylation of hydroxy groups allowed their GC-MS determination as the formation of methoxy groups provided characteristic ions in the mass spectra that indicated the location of the original hydroxy groups.[7] In addition, the utilization of commercial standards and GC-MS techniques enabled the identification of GC peaks associated with underivatized hydroxy fatty acid methyl esters (FAME).[8] However, both earlier studies employed hydrogenation to simplify the chromatograms,[7,8] which eliminated any information regarding the position of double bonds that would be particularly important in the study of reaction mechanisms.

Dr. W. Xia, Prof. S. M. Budge
Department of Process Engineering and Applied Science
Dalhousie University
Halifax NS B3H 4R2, Canada
E-mail: wei.xia@dal.ca

The ORCID identification number(s) for the author(s) of this article can be found under https://doi.org/10.1002/ejlt.201700313.

DOI: 10.1002/ejlt.201700313

 © 2017 WILEY-VCH Verlag GmbH & Co. KGaA, Weinheim

Here, we report our observations on the formation of hydroxy FA during the oxidation of edible oils through a GC-MS approach. The objective of this work was to develop a GC-MS method with sufficient resolution to allow the characterization and quantification of unsaturated hydroxy FA. We accomplished this through the use of methylation and trimethylsilyl (TMS) derivatization, fractionation with solid phase extraction (SPE), and application of electron ionization (EI) and positive chemical ionization (PCI) techniques. Several EI mass spectra of TMS derivatives of hydroxy FA have been reported in a previous study and their fragmentation rules were discussed.[9] We followed those rules and present our description of both saturated and unsaturated hydroxy FA derived from canola oil and sunflower oil. PCI studies of hydroxy FA have been limited in the literature, especially of allylic and conjugated structures. In this paper, we present the EI and methane PCI spectra of TMS derivatives of hydroxy FA and characterize their mass spectra with diagnostic ions.

2. Experimental Section

2.1. Chemicals and Standards

N,O-bis (trimethylsilyl) trifluoroacetamide (BSTFA) (>99%, for GC derivatization), sodium methoxide solution (0.5 M CH_3ONa in methanol), methyl 12-hydroxystearate (>99%), and methyl ricinoleate (>99%, methyl 12-hydroxyoctadec-*cis*-9-enoate) were purchased from Sigma–Aldrich Inc. (St. Louis, MO, US). (S)-13-HODE ((S)-13-hydroxyoctadeca-9,11-dienoic acid) methyl ester (>98%) and hydroxy linoleins (>98%, a mixture of OH-C18:2 isomers derived from trilinolein) were obtained from Cayman Chemical Company (Ann Arbor, Michigan, US). Si gel 40 (35–70 mesh) from Fluka Analytical (Switzerland) was used for SPE.

2.2. Oils and Oxidation Conditions

Sunflower and canola oils were obtained from local markets. Their proportions of the major FA in each oil (**Table 1**) were determined by transmethylation as described below. The oils (30 g) were weighed into 100 mL beakers and oxidized in the dark at 70 °C for 7 days.

Table 1. Fatty acid composition (%, w/w) of the oils.

Fatty acid	Sunflower oil (mean ± SD)	Canola oil (mean ± SD)
C16:0	5.89 ± 0.02	3.65 ± 0.02
C18:0	3.28 ± 0.00[a]	1.75 ± 0.00[b]
C18:1n-7	0.60 ± 0.01	3.10 ± 0.02
C18:1n-9	34.34 ± 0.02	59.76 ± 0.02
C18:2n-6	53.87 ± 0.01	18.39 ± 0.01
C18:3n-3	0.08 ± 0.00[c]	9.35 ± 0.00[d]
Others	1.94	4.00

[a]SD=0.004; [b]SD=0.004; [c]SD=0.001; [d]SD=0.001.

2.3. Transmethylation

Transmethylation with sodium methoxide was carried out at room temperature following the procedures described in a previous study.[10] Aliquots of 100 mg of oil (or 50 μg of hydroxy linolein) were placed into 10 mL test tubes to which was added 1 mL of *tert*-butyl methyl ether and 0.5 mL of 0.2 M sodium methoxide in methanol. The test tubes were shaken for 1 min and left still for 2 min. Then 0.1 mL of 0.5 M sulfuric acid in water was added, followed by addition of 1.5 mL of water. After vigorous shaking and centrifugation, the organic layer containing FAME was collected, and the solvent was evaporated under nitrogen.

2.4. SPE Conditions

After transmethylation, 4–20 mg of FAME obtained in section 2.3 was dissolved in 1 mL of 98:2 hexane: ethyl ether for SPE using a self-packed silica column. The silica column was prepared by filling a Pasteur pipette with 1 g of activated Si gel. A three-step SPE approach was used for extraction of hydroxy FAME.[11] The non-polar fraction was eluted using 15 mL of 98:2 hexane: ethyl ether. Then Polar Fraction 1, which contained epoxy FAME, was removed from the silica column using 15 mL of 90:10 hexane: ethyl ether. Polar Fraction 2, containing hydroxy FAME, was eluted last using 30 mL of ethyl ether.

2.5. TMS Derivatization

Both polar fractions collected in section 2.4 was evaporated to dryness under nitrogen, mixed with 50 μL BSTFA and 50 μL pyridine, and left to sit for 30 min at room temperature. After the reaction, the sample was again evaporated to dryness and then dissolved in 200 μL hexane for GC analysis. To ensure that the reaction went to completion, the hydroxy FAME standards were carried through the process and examined by GC-MS; the absence of the original standards in the chromatograms indicated that the hydroxy FAME were fully converted into their corresponding TMS ethers.

Polar Fraction 2 contained hydroxy FAME and was analyzed for the purpose of characterization of hydroxy FAME. Polar Fraction 1 was expected to contain mainly epoxy FAME and thus was not of interest in this study. The aim of derivatization of Polar Fraction 1 was to examine if any hydroxy products were collected in that fraction. Epoxy FAME remain stable during TMS derivatization because silylating reagents can only react with the functional groups possessing active hydrogens,[12] such as hydroxy groups (-OH). Therefore, TMS derivatization selectively converts hydroxy FAME into TMS ethers.

2.6. GC-MS Instrumentation

2.6.1. GC Conditions

A Trace GC Ultra gas chromatography coupled with a PolarisQ ion trap mass spectrometer was used for analysis. Four GC capillary columns were used to attempt the separation of TMS

© 2017 WILEY-VCH Verlag GmbH & Co. KGaA, Weinheim

derivatives of hydroxy FA: DB-1 ms (100% dimethylpolysiloxane, 30 m × 0.25 mm, 0.25 μm), ZB-35HT (35%-phenyl-65%-dimethylpolysiloxane, 30 m × 0.25 mm, 0.25 μm), DB-23 ((50%-cyanopropyl)-methylpolysiloxane, 30 m × 0.25 mm, 0.25 μm), and Rtx-2330 (90% biscyanopropyl/10% phenylcyanopropyl polysiloxane, 105 m × 0.25 mm, 0.2 μm). The temperature programs were modified empirically: an initial temperature program started at 60 °C and gradually increased to the end temperature that was at least 15 °C below the upper limit of the operating temperature range of the GC column. Following an initial run, the temperature program was modified by adjusting the ramp rate and hold-up time based on the resolution of the GC peaks. The temperature programs optimized for the above four GC columns were the following:

DB-1 ms: started at 60 °C and held for 2 min, increased to 180 °C at 12 °C min^{-1} and held for 5 min, increased to 225 °C at 2 °C min^{-1} and held for 10 min, increased to 300 °C at 10 ° C min^{-1} and held for 10 min with a total time of 67 min. The carrier gas was helium at 1.2 mL min^{-1}, with the injector at 280 °C in splitless mode and MS transfer line at 310 °C.

ZB-35HT: started at 60 °C and held for 2 min, increased to 180 °C at 12 °C min^{-1}, then increased to 215 °C at 2.5 °C min^{-1} and held for 20 min, increased to 300 °C at 10 °C min^{-1} and held for 10 min with a total time of 64.5 min. The carrier gas was helium at 1.4 mL min^{-1}, with the injector at 280 °C in splitless mode and MS transfer line at 310 °C.

DB-23: started at 50 °C and held for 2 min, increased to 165 °C at 15 °C min^{-1} and held for 15 min, then increased to 205 °C at 10 °C min^{-1} and held for 10 min, increased to 230 °C at 10 °C min^{-1} and held for 10 min with a total time of 51.17 min. The carrier gas was helium at 1.2 mL min^{-1}, with the injector 250 °C in splitless mode and MS transfer line at 235 °C.

Rtx-2330: started at 50 °C and held for 2 min, increased to 240 °C at 15 °C min^{-1} and held for 35 min, with a total time of 49.67 min. The carrier gas was helium at 1.0 mL min^{-1}, with the injector at 250 °C in splitless mode and MS transfer line at 245 °C.

2.6.2. MS Parameters

In EI mode, the ion source was kept at 200 °C and emission current was at 250 μA, with a mass scan range of 60–500 and ionization voltage at 70 eV. For PCI analysis, methane was used as the reagent gas at 1.5 mL min^{-1} and the parameters remained the same as EI.

Methyl 12-hydroxystearate, methyl ricinoleate, and (S)-13-HODE methyl ester were used as references for the retention times and fragmentation patterns of OH-C18:0, OH-C18:1, and OH-C18:2. Transmethylation of the hydroxy linolein standard produced methyl esters of both 13-hydroxyoctadeca-9,11-dienoic acid and 9-hydroxyoctadeca-10,12-dienoic acid for the confirmation of the retention times and mass spectra of OH-C18:2 found in oxidized oils. Further assignments of the other peaks were made according to the rules reported in the previous study.[9]

3. Results and Discussion

3.1. GC Column Selection and Patterns of Hydroxy FA

In this paper, all hydroxy FA are discussed as methyl esters in their TMS ether forms, where the original hydroxy groups were converted into trimethylsiloxy (OTMS) groups. The following aspects were taken into consideration: 1) DB-1 ms and ZB-HT35 were not able to resolve the TMS derivatives of hydroxy FAME from other unidentified non-TMS compounds; thus, the interferences from unknown peaks prevented conclusive identification and quantification of hydroxy FAME and 2) Rtx-2330 showed equivalency to DB-23 in separation of the hydroxy FAME from other polar compounds, but it did not allow the separation of 9-OH and 10-OH-C18:0 from the isomers of OH-C18:1; therefore, DB-23 was considered superior to Rtx-2330. However, none of the columns could completely resolve all positional isomers of allylic OH-C18:1 (C8, 9, 10, 11-substituted positional isomers). Therefore, DB-23 showed the best separation for quantitative purposes, although the allylic OH-C18:1 isomers co-eluted with each other.

Hydroxy FA with the same structures and retention times were found in both fresh and oxidized canola and sunflower oils (total ion chromatograms shown for canola oil in **Figure 1**, entire chromatograms in Figure S1, Supporting Information, with peak identities in **Table 2**), with the exception of 15-hydroxyoctadeca-9,12-dienoic acid (Peak 4) that was not found in sunflower oil but was present in canola oil. The hydroxy FA

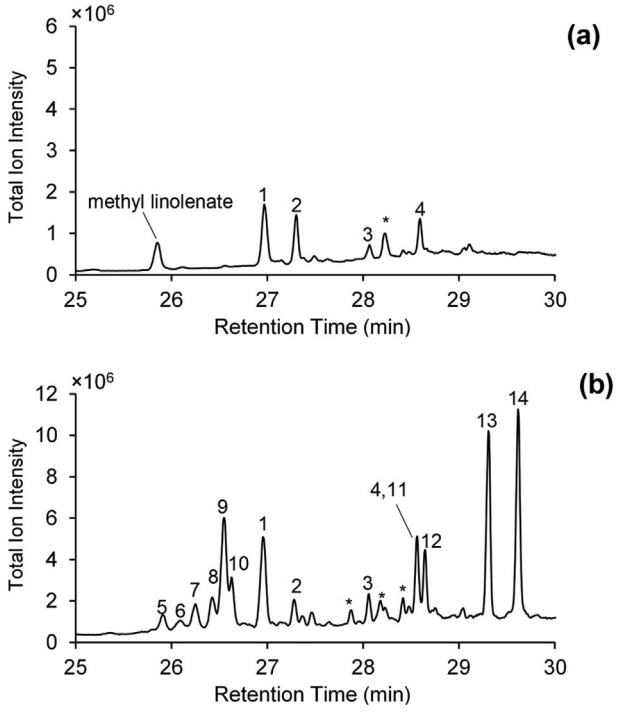

Figure 1. Total ion chromatograms of TMS ethers of hydroxy FAME derived from fresh canola oil (a) and oxidized canola oil (b), obtained using a DB-23 capillary column. Oxidation conditions: 70 °C, 7 days, in dark. *represents unidentified hydroxy compounds.

© 2017 WILEY-VCH Verlag GmbH & Co. KGaA, Weinheim

Table 2. Characteristic EI spectral ions (% relative abundance) corresponding to the identified compounds in Figures 1 and 2.

Compound (in TMS ether form)	Peak no.	Molecular weight	Characteristic EI spectral ions *m/z* (% relative abundance)
OH-C18:0			
Methyl 9-hydroxyoctadecanoate	1[a]	386	371 (4), 339 (22), 259 (100), 229 (29), 155 (68)
Methyl 10-hydroxyoctadecanoate	1[a]	386	371 (4), 339 (12), 273 (100), 215 (28), 169 (30)
OH-C18:1			
Methyl 12-hydroxyoctadec-9-enoate	2	384	369 (6), 337 (20), 299 (14), 270 (54), 187 (100)
Methyl 8-hydroxyoctadec-9-enoate	5,8	384	369 (2), 337 (10), 241 (100), 129 (52)
Methyl 9-hydroxyoctadec-10-enoate	6[b],9[b]	384	369 (2), 337 (8), 227 (100), 129 (62)
Methyl 10-hydroxyoctadec-8-enoate	6[b],9[b]	384	369 (2), 337 (12), 271 (100), 149 (80)
Methyl 11-hydroxyoctadec-9-enoate	7,10	384	369 (2), 337 (7), 285 (100), 163 (50)
OH-C18:2			
Methyl 15-hydroxyoctadeca-9,12-dienoate	4[c]	382	335 (7), 310 (67), 145 (85), 73 (100)
Methyl 13-hydroxyoctadeca-9,11-dienoate	11[c],14	382	382 (M^+, 40), 367 (4), 335 (7), 311(100), 225 (40)
Methyl 9-hydroxyoctadeca-10,12-dienoate	12,13	382	382 (M^+, 42), 367 (2), 311(30), 225 (100)
diOH-C18:0			
Methyl 9,10-dihydroxyoctadecanoate	3	474	332 (28), 259 (100), 215 (30), 155 (83)
Epoxy-OH-C18:1			
Methyl 9,10-epoxy-11-hydroxyoctadec-12-enoate	-[d]	398	383 (3), 241 (11), 199 (100)
Methyl 12,13-epoxy-11-hydroxyoctadec-9-enoate	-[d]	398	383 (2), 327 (10), 285 (100)

[a]Methyl 9-hydroxyoctadecanoate co-eluted with methyl 10-hydroxyoctadecanoate at Peak 1; [b]The *trans/cis* isomer of methyl 10-hydroxyoctadec-8-enoate co-eluted with the *trans/cis* isomer of methyl 9-hydroxyoctadec-10-enoate at Peak 6 and Peak 9; [c]Methyl 15-hydroxyoctadeca-9,12-dienoate (Peak 4) co-eluted with an isomer of methyl 13-hydro xyoctadeca-9,11-dienoate (Peak 11); [d]The TMS ethers of methyl 9,10-epoxy-11-hydroxyoctadec-12-enoate and methyl 12,13-epoxy-11-hydroxyoctadec-9-enoate are labelled as 11-OTMS-9,10-epoxyoctadec-12-enoate and 11-OTMS-12,13-epoxyoctadec-9-enoate in **Figure 2**, respectively.

with Peak No. 1–4 (Figure 1) found in fresh canola oil did not have allylic hydroxy groups (note: only Peak 1–3 shown in sunflower oil). It is speculated that the non-allylic hydroxy FA, such as ricinoleic acid (Peak 2),[13,14] are formed naturally through enzymatic processes in seed plants, although such an inference needs further proof.

The 15-hydroxyoctadeca-9,12-dienoic acid co-eluted with a 13-hydroxyoctadeca-9,11-dienoic acid isomer and could not be separated using any of the four GC columns. The mono-unsaturated hydroxy FA were present in both *cis* and *trans* forms; therefore, each OH-C18:1 positional isomer occurred as two geometric isomers. Also, both 13-hydroxyoctadeca-9,11-dienoic acid and 9-hydroxyoctadeca-10,12-dienoic acid had two geometric isomers and thus appeared as four peaks in chromatograms (Figure 1b). The two geometric isomers of OH-C18:2 were likely *cis/trans* and *trans/trans* structures, according to a previous study determining hydroxydienes.[15] Although it was inferred that the *trans* isomers would elute before their *cis* isomers on the GC column employed, further tests should be conducted to confirm the identities of these hydroxy FA. The geometric isomers could not be differentiated by their EI or PCI spectra.

In terms of the resolution of epoxy-hydroxy FA, only DB-23 and Rtx-2330 were compared for their performances, with the Rtx-2330 having slightly better performance due to its highly polar phase. However, co-elution of peaks still occurred with Rtx-2330 (Figure 2a, with entire chromatogram in Figure S2, Supporting Information). The identification of the epoxy-hydroxy structures was based on the comparison with the mass spectra shown in a previous report of the homolytic decomposition of linoleic hydroperoxides (13-hydroperoxyoctadeca-*cis*-9, *trans*-11-dienoic acid and 9-hydroperoxyoctadeca-*cis*-12,*trans*-10-dienoic acid).[4] Several peaks had identical mass spectra, confirming the presence of epoxy-hydroxy stereoisomers. Possible geometric isomers would include *cis*/*trans* epoxy and *cis*/*trans* double bonds in their structures. Also, stereoisomers of 12,13-epoxy-11-hydroxyoctadec-9-enoic acid (*erythro*- and *threo*-configurations) have been identified as decomposition products from 13L-hydroperoxyoctadeca-9,11-dienoic acid in the presence of hemoglobin.[6] The presence of such stereoisomers cannot be excluded. However, due to the co-elution of the epoxy-hydroxy isomers and interferences from other unknown compounds, it is difficult to determine the number of geometric isomers found for either of 9,10-epoxy-11-hydroxyoctadec-12-enoic acid and 12,13-epoxy-11-hydroxyoctadec-9-enoic acid. In future studies, an alternative method is necessary to describe the number of geometric isomers of epoxy-hydroxy FA derived from oils. GC-MS alone would not distinguish the geometric structures.

Although the hydroxy FAME were mainly present in Polar Fraction 2, small signals associated with epoxy-hydroxy FAME were found in Polar Fraction 1, indicating that a small amount of epoxy-hydroxy FAME was collected in that fraction. Therefore, future studies quantifying these epoxy-hydroxy FA should first optimizing the SPE conditions to allow better separation between epoxy FAME and epoxy-hydroxy FAME. Signals associated with mono- and di-hydroxy FA were absent in Polar Fraction 1.

© 2017 WILEY-VCH Verlag GmbH & Co. KGaA, Weinheim

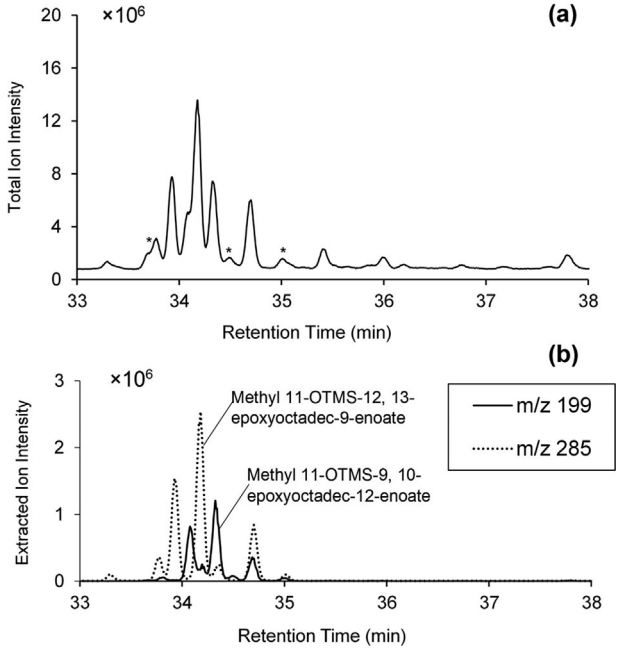

Figure 2. Total ion chromatogram (a) and single ion chromatogram (b) of TMS ethers of epoxy-hydroxy fatty acids derived from oxidized sunflower oil using an Rtx-2330 capillary column. The single ion chromatograms were plotted by monitoring *m/z* 199 and 285 for methyl 11-OTMS-9, 10-epoxyoctadec-12-enoate and 11-OTMS-12,13-epoxyoctadec-9-enoate, respectively. *represents unknown peaks which caused interferences.

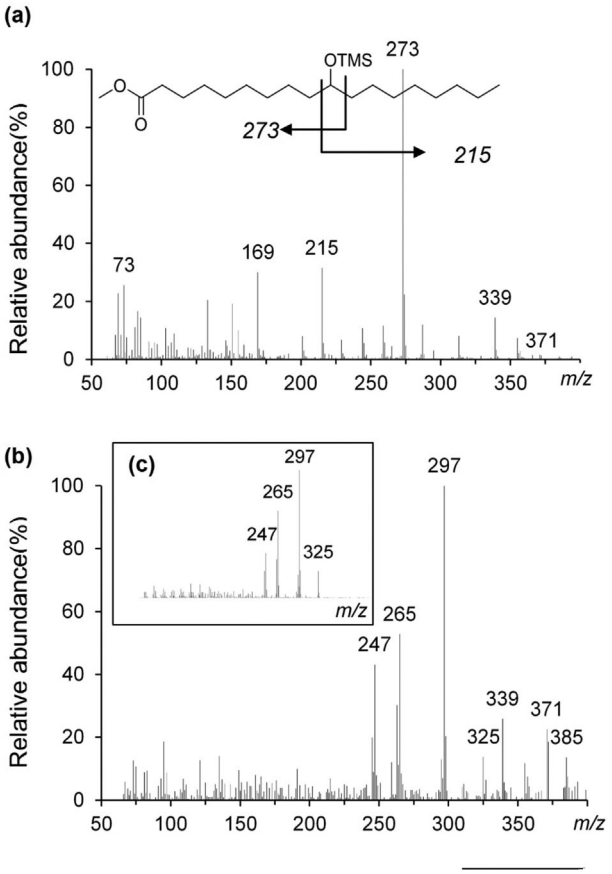

Figure 3. EI (a) and PCI (b) spectra of methyl 10-OTMS-octadecanoate (molecular mass: 386). PCI (c) spectrum of methyl oleate. CI reagent gas: methane at 1.5 mL min^{-1}.

3.2. GC-MS Characterization of Hydroxy FA

3.2.1. Saturated OH-FAME

In EI mass spectra, *m/z* 73 ($[(CH_3)_3Si]^+$) and *m/z* 75 ($[(CH_3)_2SiOH]^+$) are diagnostic ions for TMS ethers,[12] indicating the presence of a hydroxy group in the original FAME and differentiating the identities of hydroxy FAME from other polar FAME. Molecular ions are not detectable; therefore, a $[M\text{-}15]^+$ ion, generated from a loss of a methyl moiety, is normally used as an indication of the molecular mass.[12] In addition, a few intense ions in EI spectra can normally be used to determine the location of the OTMS in the FA chain, which represents the hydroxy group.

Specifically, the cleavage α to the OTMS moiety results in characteristic ions in EI spectra. For example, methyl 10-OTMS-octadecanoate, or 10-OH-C18:0, is identified by the two ions (*m/z* 215 and 273) resulting from α-cleavage occurring on both sides of the carbon where the OTMS groups is bonded. However, it was also noticed that *m/z* 371, although being the $[M\text{-}15]^+$ ion, was weak in the spectrum (**Figure 3**a).

PCI spectra do not differentiate between structural isomerism. Therefore, methyl 9-OTMS, 10-OTMS, and 12-OTMS-octadecanoate gave the same PCI spectra (Figure 3b), with the major ions being *m/z* 385 $[M\text{-}1]^+$, 371 $[M\text{-}15]^+$, 339 $[M+H\text{-}48]^+$, 325 $[M+C_2H_5\text{-}90]^+$, 297 $[M+H\text{-}90]^+$, 265 $[297\text{–}32]^+$, and 247 $[265\text{–}18]^+$. In the PCI spectra of saturated structures containing TMS ethers, the expected ion $[M+1]^+$ was not detectable; instead, $[M\text{-}1]^+$ at *m/z* 385 was present, while *m/z* 371, the $[M\text{-}15]^+$ ion, was abundant (21% of the base peak) and could be used to determine the molecular mass of the peak. The base peak in the PCI spectrum was *m/z* 297 $[M+H\text{-}90]^+$, produced by the loss of a $[(CH_3)_3SiOH]^+$ moiety from the molecule.[16] It should be noted that, in the PCI spectra of the TMS ethers of OH-C18:0, the relative intensities of *m/z* 325, 297, 265, and 247 resembled those in the PCI spectrum of methyl oleate (Figure 3c).

The PCI spectrum of methyl 12-OTMS-octadecanoate has been reported using isobutane as the reagent gas,[16] where weak signals were reported for $[M+H]^+$, $[M\text{-}H]^+$, $[M+H\text{-}15]^+$, and $[M\text{-}H\text{-}15]^+$, with all at ≈3–5% of the base peak *m/z* 297 $[M+H\text{-}90]^+$. Its PCI spectrum with ammonia as reagent gas also gave an abundant *m/z* 297 $[M+H\text{-}90]^+$, with intense ions at *m/z* 314 $[M+NH_4\text{-}90]^+$, 387 $[M+H]^+$, and 404 $[M+NH_4]^+$ in the spectrum. Both of those studies identified the primarily protonated molecules $[M+H]^+$ arising from proton transfer and expected with PCI; however, in the present work, $[M+H]^+$ generated in the PCI spectrum of methyl 12-OTMS-octadecanoate with methane was less than 1% in relative intensity. Methane has the lowest proton affinity (PA) (546.0 kJ mol^{-1} for CH_5^+ and 684.1 kJ mol^{-1} for $C_2H_5^+$) among the three reagent gases discussed here (823.8 kJ mol^{-1} for isobutane reactant ion $C_4H_9^+$, 857.7 kJ mol^{-1} for ammonia reactant ions NH_4^+).[17] The molecules protonated with methane (CH_5^+ and $C_2H_5^+$)

© 2017 WILEY-VCH Verlag GmbH & Co. KGaA, Weinheim

had higher internal energy than those with isobutane and ammonia, which is determined by the difference of the PA between the molecules and the reagent gas,[18] so PCI with methane produced more fragmentation than isobutane and ammonia, resulting in less intense $[M+H]^+$ ions. In addition, the high hydride ion affinities (HIA) of methane (1130 kJ mol^{-1} for CH_5^+ and 1138 kJ mol^{-1} for $C_2H_5^+$) and isobutane (967 kJ mol^{-1} for isobutane reactant ions $C_4H_9^+$), compared to ammonia (816 kJ mol^{-1} for ammonia reactant ions NH_4^+),[17] facilitated the formation of deprotonated molecules and thus explained the presence of $[M\text{-}H]^+$ in the spectra. Therefore, the high HIA and low PA of methane produced a high degree of fragmentation, a relatively small $[M+H]^+$, and a visible $[M\text{-}H]^+$ in PCI spectra.

The collision-stabilized complexes ($[M+29]^+$ and $[M+41]^+$), which are normally seen in methane PCI spectra, were not observed for the TMS derivatives. However, *m/z* 325 $[M+29]^+$ was clear in the PCI spectrum of methyl oleate (Figure 3c) under the same PCI conditions.

3.2.2. Mono-Unsaturated OH-FAME

3.2.2.1. Non-Allylic Structures

In the non-allylic structure, where the OTMS group is separated from a double bond by at least one carbon atom, the α-cleavage resembled that occurring in saturated OH-FAME. For example, α-cleavage in methyl 12-OTMS-octadec-9-enoate (TMS ether of methyl ricinoleate) resulted in *m/z* 187 and *m/z* 299 (Figure S3a, Supporting Information). However, an abundant ion of even numbered mass was also found at *m/z* 270; this is known as the "migration ion" ($CH_3O(TMSO)C^+(CH_2)_7CH=CH\text{-}CH_2$) and is formed by transferring the TMS group to the ester group and cleaving between C11 and C12 [9]. Because of the even numbered mass, it is distinct from the other major ions in spectra.

The PCI spectrum of the same structure showed major ions at *m/z* 383 $[M\text{-}1]^+$, 369 $[M\text{-}15]^+$, 337 $[M+H\text{-}48]^+$, 295 $[M+H\text{-}90]^+$, 263, and 245 (Figure S3b, Supporting Information). Compared to the PCI spectra of the saturated structures, the base peak shifted to $[M\text{-}15]^+$, providing an indication of the molecular weight.

3.2.2.2. Allylic Structures

When the OTMS group was bonded to an allylic carbon, α-cleavage still resulted in the base ion in EI spectra[9]; however, the α-cleavage between the OTMS group and the double bond was not observed. For instance, *m/z* 241 was the base ion in the spectrum of 8-OTMS-octadec-9-enoate and the ion resulting from the cleavage between C8 and C9 was not detectable (Figure S4a, Supporting Information). The ion *m/z* 369 $[M\text{-}15]^+$ was present but at less than 10% intensity.

Again, the positional isomers of TMS-derivatized allylic OH-C18:1 could not be differentiated from each other by their PCI spectra. However, the base ion was *m/z* 263 (Figure S4b, Supporting Information), different from the non-allylic structures (Figure S3b, Supporting Information). It should be noted that the $[M\text{-}15]^+$ ion in the PCI spectra was much less intense for all of the allylic structures, while it was often the base ion for non-allylic structures. The PCI spectrum of 8-OTMS-octadec-9-enoate still gave an ion of *m/z* 295 $[M+H\text{-}90]^+$, but *m/z* 293 was more intense. The presence of *m/z* 293, 263, and 245 was similar to those shown in the PCI spectrum of methyl linoleate (Figure S4c, Supporting Information).

3.2.3. Di-Unsaturated OH-FAME

3.2.3.1. Non-Conjugated Structures

The only non-conjugated OH-C18:2 identified here was methyl 15-OTMS-octadeca-9,12-dienoate. Its EI spectrum showed two diagnostic ions, *m/z* 145 and 310, with no molecular ion observed (Figure S5a, Supporting Information). The α-cleavage occurred on both sides of the OTMS group, producing *m/z* 145 and 339.[19] As described above for the non-allylic structure (methyl 12-OTMS-octadec-9-enoate), a migration ion can form from the fragment containing the ester group; therefore, *m/z* 310 was generated from a migration ion ($CH_3O(TMSO)C^+(CH_2)_7CH=CH\text{-}CH_2\text{-}CH=CH\text{-}CH_2$) with cleavage between C14 and C15.

The PCI spectrum of methyl 15-OTMS-octadeca-9,12-dienoate gave a base peak of *m/z* 293 $[M+H\text{-}90]^+$, with other major ions found at *m/z* 381$[M\text{-}H]^+$, 367 $[M\text{-}15]^+$, 335 $[M\text{-}48]^+$, 261, and 243. The peaks of *m/z* 293, 261, and 243 were also found in the PCI spectrum of methyl linolenate (Figure S6c, Supporting Information); however, ions of *m/z* 367 and 381 in the PCI spectrum of 15-OTMS-octadeca-9,12-dienoate distinguished it from methyl linolenate. Therefore, the presence of *m/z* 293, 261, and 243 in the PCI spectrum of 15-OTMS-octadeca-9,12-dienoate was consistent with the finding that the major peaks appearing between *m/z* 240–300 in PCI spectra of TMS-hydroxy FAME were similar to those of regular FAME with one more site of unsaturation. This finding will facilitate deduction of the degree of unsaturation in hydroxy FA.

3.2.3.2. Conjugated Dienes

Two conjugated OH-C18:2, 9-hydroxyoctadeca-10,12-dienoic acid and 13-hydroxyoctadeca-9,11-dienoic acid, were found in oxidized oils. The EI spectra of the conjugated structures are characteristic due to the base ions,[20] which resulted from the α-cleavage to the OTMS group occurring on the opposite side of the double bonds (Figure S6a, Supporting Information). No cleavage was observable between the OTMS group and the conjugated double bonds. Moreover, the conjugated system, including the two double bonds and the OTMS group, was cleaved as a whole fragment (Figure S6a, Supporting Information). This finding was consistent with the previous fragmentation patterns reported by Kleiman and Spencer.[9] Taking methyl 9-OTMS-octadeca-10,12-dienoate as an example, *m/z* 225 was the base ion in the EI spectrum, formed by cleavage between C8 and C9. The fragment of *m/z* 225 contained the OTMS group as well as the conjugated double bonds. Cleavage between C13 and

© 2017 WILEY-VCH Verlag GmbH & Co. KGaA, Weinheim

C14 produced *m/z* 311, which also contained the conjugated system. In addition, the conjugated structures gave a clear molecular ion at *m/z* 382 and an obvious *m/z* 367 $[M\text{-}15]^+$, distinct from the EI spectra of other structures mentioned above.

The PCI spectra of methyl 9-OTMS-octadeca-10,12-dienoate and 13-OTMS-octadeca-9,11-dienoate were not distinguishable from each other and were quite similar to that of non-conjugated methyl 15-OTMS-octadeca-9,12-dienoate (Figure S5b, Supporting Information). For instance, both conjugated structures had *m/z* 321, 261, and 243, with a base peak of *m/z* 293 $[M + H\text{-}90]^+$ (Figure S6b, Supporting Information), which resembled the major peaks found in the PCI spectrum of methyl linolenate (Figure S6c, Supporting Information). However, there were a number of ions that differentiated the conjugated and non-conjugated structures. Specifically, the PCI spectra of the conjugated diene structures showed a larger $[M + H]^+$ than $[M\text{-}H]^+$, while the opposite was observed for the other structures discussed above. Moreover, the conjugated diene structures produced a more intense *m/z* 321 than *m/z* 335 in the PCI spectra, while methyl 15-OTMS-octadeca-9,12-dienoate showed the opposite pattern. Last, as observed for OH-C18:1, the non-conjugated/non-allylic structures gave a substantially stronger *m/z* 367 $[M\text{-}15]^+$ in PCI spectra than the conjugated/allylic structures.

3.2.4. diOH-FAME

A dihydroxy FA was identified as 9,10-dihydroxyoctadecanoic acid. In the EI spectrum of methyl 9,10-diOTMS-octadecanoate, neither the molecular ion nor the $[M\text{-}15]^+$ was visible, making it difficult to interpret the molecular weight (Figure S7a, Supporting Information). However, the PCI spectrum of this compound indicated the molecular weight (MW: 474) by *m/z* 459 $[M\text{-}15]^+$ and a small but visible *m/z* 473 $[M\text{-}H]^+$ (Figure S7b, Supporting Information). In the EI spectrum, the α-cleavage between C9 and C10 was shown by *m/z* 215 and 259 (Figure S7a, Supporting Information). The ion *m/z* 361, resulting from the cleavage between C10 and C11, was not visible in the spectrum; however, its migration ion *m/z* 332 ($CH_3O(TMSO)C^+(CH_2)_7CH$-(OTMS)),[9] as an even numbered ion, was distinct from other ions.

3.2.5. Epoxy-Hydroxy FAME

Epoxy-hydroxy FA found in Polar Fraction 2 have been reported to form from linoleic acid hydroperoxides.[4] In the oxidized oils (Figure 2), a group of peaks were identified as isomers of methyl 11-OTMS-9,10-epoxyoctadec-12-enoate and 11-OTMS-12,13-epoxyoctadec-9-enoate. The base peaks in the EI spectra of methyl 11-OTMS-9,10-epoxyoctadec-12-enoate (Figure S8a, Supporting Information) and 11-OTMS-12,13-epoxyoctadec-9-enoate (Figure S9a, Supporting Information) were *m/z* 199 and 285, respectively, produced from α-cleavage occurring between the OTMS group and the epoxy group. Cleavage also occurred on the other side of the epoxy group, resulting in a significantly weaker ion in the high mass range: *m/z* 241 for 11-OTMS-9,10-epoxyoctadec-12-enoate and *m/z* 327 for 11-OTMS-12,13-epoxyoctadec-9-enoate. In both EI spectra, *m/z* 383 $[M\text{-}15]^+$ was visible but at extremely low intensity. The PCI spectra of these two structures were difficult to interpret (Figures S8b and S9b, Supporting Information). Both showed *m/z* 383 $[M\text{-}15]^+$ to allow determination of molecular weight; however, much more fragmentation was found for epoxy-hydroxy structures in methane PCI spectra. The 11-hydroxy-12,13-epoxyoctadec-9-enoic acid and 11-hydroxy-12,13-epoxyoctadec-9-enoic acid observed in this study were possibly formed from 9-hydroperoxy-C18:2 and 13-hydroperoxy-C18:2.[21]

4. Conclusion

This work identified both saturated and unsaturated hydroxy FA as lipid oxidation products in edible oils using GC-MS analysis of their TMS derivatives and evaluation of the EI and PCI spectra. In general, EI is a hard ionization method and results in high fragmentation so it generates more characteristic ions that are useful in differentiating the positional isomers of hydroxy FA but often failed to provide information regarding the molecular weights. In contrast, PCI is a soft ionization technique so less fragmentation is achieved. With methane as the reagent gas, PCI provides less structural information from fragmentation patterns but can confirm the molecular weights of the TMS derivatized compounds with $[M\text{-}15]^+$, as well as the number of double bonds involved in the structure. It is clear that EI spectra provide more detailed structural information; however, when the information regarding molecular weights is unclear, PCI becomes a useful alternative.

The fragmentation patterns of hydroxy FA in their TMS ether forms in EI are summarized as follows:

1) In EI spectra, a saturated monohydroxy FA is readily interpreted by the two ions produced from the α-cleavage on both sides of the OTMS group;
2) Interpretation of unsaturated hydroxy FA can proceed by first distinguishing non-allylic and allylic structures: A non-allylic structure produces two fragments by α-cleavage on both sides of the OTMS group, with a migration ion generated from the fragment with the ester group. The migration ion is easily found as the only even numbered ion with a relatively high intensity in the spectrum. The non-allylic structures encountered in this study have only one methylene group between the hydroxy group and the double bond; therefore, the presence of the migration ion and the other fragment ion produced from the α-cleavage enables deduction of the structure of the hydroxy FA;
3) Allylic structures, including conjugated dienes, always show base peaks resulting from the α-cleavage of OTMS group on the side opposite to the double bond(s). The allylic system is cleaved as a whole, without cleavage between the OTMS group and the double bond(s);
4) The number of epoxy-hydroxy structures encountered in this work is limited. Both compounds gave base peaks derived from the cleavage between the OTMS group and the epoxy group. As the OTMS group was allylic to the

© 2017 WILEY-VCH Verlag GmbH & Co. KGaA, Weinheim

double bond, no cleavage was found between the allylic carbons.

The findings with PCI are summarized as follows:

1) $[M+H]^+$ and $[M\text{-}H]^+$ are both present for most of the TMS derivatives of hydroxy FA found in this work; thus, $[M+H]^+$ and $[M\text{-}H]^+$, as well as $[M+H\text{-}90]^+$, are useful indicators of molecular weight;
2) PCI spectra of hydroxy FA cannot differentiate positional isomers; however, the intensities of the major ions vary in allylic structures and non-allylic structures. Non-allylic structures tend to give an intense $[M\text{-}15]^+$ ion in the PCI spectrum, often larger than 90% of the base peak, in contrast to allylic/conjugated structures;
3) Apart from the $[M+H]^+$, $[M\text{-}H]^+$, and $[M\text{-}15]^+$ ions, the major ions shown between *m/z* 240–300 in the PCI spectra of TMS ethers of hydroxy FAME resembled those ions in the PCI spectra of regular FAME with one more site of unsaturation. For example, the major ions in the PCI spectra of OH-C18:0 resembled the ions observed for methyl oleate. The only exception was ricinoleic acid (12-hydroxyoctadec-9-enoic acid), which gave *m/z* 295, 263, 245 but PCI spectra of methyl linoleate had three intense ions at *m/z* 293, 263, 245.

By avoiding hydrogenation and applying these fragmentation patterns, we were able to characterize the structures of several unsaturated hydroxy FAME derived from oxidation of canola and sunflower oils.

The mono-unsaturated hydroxy FA formed during lipid oxidation in the oils were mainly 8-, 9-, 10-, and 11-substituted, with di-unsaturated hydroxy FA being mostly 9- and 13-substituted. The GC peaks associated with OH-C18:1 were visibly less abundant in oxidized sunflower oils than oxidized canola oil, which may be due to the lower abundance of oleic acid (C18:1) in sunflower oil than canola oil. However, the work presented in this manuscript is a qualitative study; quantitative measurements were not conducted. Further comparison of the concentrations of hydroxy FA between sunflower and canola oils should be carried out. Our identification of these unsaturated hydroxy FA is a prerequisite for such quantitative work. Since this research focused on hydroxy FA, other oxidized FA were not involved. Future work can modify the three-step SPE approach to extract and characterize other oxidized FA, such as keto FA.

Abbreviation

BSTFA, N,O-bis (trimethylsilyl) trifluoroacetamide; EI, electron ionization; FAME, fatty acid methyl ester; HIA, hydride ion affinity; HODE, hydroxyoctadecadienoic acid; MW, molecular weight; OTMS, trimethylsiloxy; PA, proton affinity; PCI, positive chemical ionization; SPE, solid phase extraction; TMS, trimethylsilyl.

Supporting Information

Supporting Information is available from the Wiley Online Library or from the author.

Conflict of Interest

The authors declare no conflict of interest.

Keywords

TMS derivatives, EI, PCI, fragmentation patterns

Received: July 19, 2017
Revised: September 21, 2017
Published online:

[1] K. M. Schaich, *Lipid Technol*. **2012**, *24*, 55.
[2] E. Choe, D. B. Min, *Comp. Rev. Food Sci. Food Safety*. **2006**, *5*, 169.
[3] K. M. Schaich, Lipid oxidation: Theoretical aspects. *Bailey's industrial oil and fat products*. (Ed: Shahidi F), Wiley, Hoboken **2005**.
[4] H. W. Gardner, R. Kleiman, D. Weisleder, *Lipids* **1974**, *9*, 696.
[5] T. A. Dix, L. J. Marnett, *J. Biol. Chem*. **1985**, *260*, 5351.
[6] M. Hamberg, *Lipids* **1975**, *10*, 87.
[7] R. Wilson, R. Smith, P. Wilson, M. J. Shepherd, R. A. Riemersma, *Anal. Biochem*. **1997**, *248*, 76.
[8] S. Marmesat, J. Velasco, M. C. Dobarganes, *J. Chromatogr. A* **2008**, *1211*, 129.
[9] R. Kleiman, G. F. Spencer, *J. Ame. Oil Chem. Soc*. **1973**, *50*, 31.
[10] J. Velasco, O. Berdeaux, G. Márquiz-Ruiz, M. C. Dobarganes, *J. Chromatogr. A* **2002**, *982*, 145.
[11] E. Mubiru, K. Shrestha, A. Papastergiadis, B. de Meulenaer, *J. Chromatogr. A* **2013**, *1318*, 217.
[12] C. F. Poole, *J. Chromatogr. A* **2013**, *1296*, 2.
[13] L. J. Morris, *Biochem. Biophys. Res. Commun*. **1967**, *29*, 311.
[14] J. L. Harwood, *Biochim. Biophys. Acta*. **1996**, *1301*, 7.
[15] A. Morales, C. Dobarganes, G. Márquiz-Ruiz, J. Velasco, *J. Ame. Oil Chem. Soc*. **2010**, *87*, 1271.
[16] R. D. Plattner, H. W. Gardner, R. Kleiman, *J. Ame. Oil Chem. Soc*. **1983**, *60*, 1298.
[17] J. B. Westmore, M. M. Alauddin, *Mass Spec. Rev*. **1986**, *5*, 381.
[18] O. D. Sparkman, Z. Penton, F. G. Kitson, *Gas chromatography and mass spectrometry a practical guide*. Elsevier, Boston **2011**.
[19] M. Hamberg, G. Hamberg, *Phytochem*. **1996**, *42*, 729.
[20] P. Spiteller, G. Spiteller, *Chem. Phys. Lipids* **1997**, *89*, 131.
[21] M. Hamberg, B. Gotthammar, *Lipids* **1973**, *8*, 737.

 © 2017 WILEY-VCH Verlag GmbH & Co. KGaA, Weinheim